Development and characterization of a 3D oral mucosa model as a tool for host-pathogen interactions

Kássia de Carvalho Dias[a,*], Denise Lins de Sousa[a], Paula Aboud Barbugli[a], Paulo Sérgio Cerri[b], Vehid Max Salih[c], Carlos Eduardo Vergani[a,*]

[a] Department of Dental Materials and Prosthodontics, Oral Rehabilitation Program, Araraquara School of Dentistry UNESP, Univ. Estadual Paulista, Centro, 14801903 Araraquara, SP, Brazil
[b] Department of Morphology, Laboratory of Histology and Embryology, Araraquara School of Dentistry UNESP, Univ. Estadual Paulista, Araraquara, SP, Brazil
[c] Plymouth University, Peninsula Schools of Medicine and Dentistry, UK

ABSTRACT

The aim of this study was to (i) design, develop and validate a practical and physiologically relevant reconstituted *in vitro* oral mucosa tissue model and (ii) to assess its applicability in *in vitro* host-pathogen interactions with *C. albicans* and *S. aureus*. Co-culture organotypic constructions were created by incorporating specific numbers of keratinocytes (NOK-si) onto cellularised, collagen gel scaffolds containing human gingival fibroblasts incubated in KGM media and cultured for 14 days. The detection of the appropriate oral mucosa/epithelial structure was evaluated by histology (hematoxylin and eosin (HE), periodic acid–Schiff (P.A.S.) and Picrosirius red), and immunocytochemistry (cytokeratin 13, cytokeratin 14, Ki-67 and collagen IV) compared to a normal human gingiva. The morphology of the reconstituted tissue was analyzed by Transmission Electron Microscopy. To further quantitate tissue damage, lactate dehydrogenase (LDH) was measured in the tissue supernatant. NOK-si grown upon a gingival scaffold provided an organotypic model in an *in vitro* setting and exhibited structural characteristics typically associated with normal oral mucosa. Immunocytochemistry revealed the detection of epithelial cytokeratins 13 and 14, Col IV and Ki-67 in the reconstituted oral mucosa model. Infection was detected after 8 h and 16 h. This study presents an *in vitro* cellularised, organotypic model of reconstituted oral mucosa, which enables close control and characterization of its structure and differentiation over a mid-length period of time in culture.

1. Introduction

Reconstituted oral mucosa tissue (ROMT) represents a model providing suitable matrix support structure in conjunction with viable cells coupled with an optimal growth environment that allow the development of functional tissue *in vitro*. The basic premise of ROMT is that controlled manipulation of the extracellular microenvironment can influence the ability of cells to organize, grow, differentiate, form a functional extracellular matrix (ECM) and, ultimately, generate new functional tissue (Scheller et al., 2009). ROMT has a broad applicability and it has been used as an alternative to human and animal testing of drugs, and for pharmacological and clinical applications (Brohem et al., 2011). Moreover, three-dimensional culture exhibits cells growing in an environment that closely mimics the *in vivo* environment (Edmondson et al., 2014).

Although the components of ROMT are basically the same, different methodologies to reconstitute epithelium and connective tissue have been reported. There is no consensus in relation to the kind of keratinocyte and fibroblast cells used to reconstitute epithelial- and connective-like layers, respectively, and a variety of scaffolds have been employed (Boelsma et al., 1999). The model proposed in this paper is composed of an epithelial- and connective-like layers formed by immortalized normal human oral keratinocytes (NOK-si), and a collagen matrix formed by human gingival fibroblasts (FGH) in a rat tail collagen type I as scaffold. The use of established cell lines allows homogeneous and unlimited access by passaging and cryopreservation and may also improve the reproducibility and consistency of 3D models, thereby allowing specific pathways or variables to be identified and assessed (Boelsma et al., 1999).

A similar oral mucosa model developed by Dongari-Bagtzoglou and

Kashleva (Dongari-Bagtzoglou & Kashleva, 2006) used a line of normal keratinocytes immortalized in a collagen and fibroblast matrix, as in the present study. However, the authors used 3T3 fibroblasts from mice in the dermal layer, which do not present the same dermal layer contraction pattern as achieved by our research group with human gingival fibroblasts, meaning our model is closer to human oral mucosa. In addition, the advantages of using stablished cell lines are that donor samples is not needed and interindividual differences do not influence experiments (Kehe et al., 1999). Furthermore, other studies that develop ROMT use the corneal dermis or even synthetic polymers as scaffolds, which also fail to adequately reproduce the desired in situ conditions. Commercial models do not always have a dermal layer and most of them are developed with tumor cell lines which do not provide the same realistic healthy oral mucosa as proposed in this study.

As a tool for host-pathogens interactions, ROMT has been used to evaluate the potential of microorganisms to grow on, penetrate and damage oral mucosa and to elucidate the mechanism of local infection. It has been suggested that *Candida albicans* improves its ability to penetrate across the oral mucosa and to promote tissue destruction leading to focal infection when it is associated with *Staphylococcus aureus* (Shirtliff et al., 2009). *C. albicans* can colonize the cavity alone or in combination with other microorganisms (Coronado-Castellote & Jiménez-Soriano, 2013), and it is the most frequently isolated microorganism (64.4%) in denture bases (Ribeiro et al., 2012). *C. albicans* has numerous virulence factors which allow it to invade and infect host cells; for example, polymorphism (Jacobsen et al., 2012; Mayer et al., 2013), presence of adhesins (Mayer et al., 2013; Garcia et al., 2011), ability to form biofilm (Mayer et al., 2013; Finkel & Mitchell, 2011), and phospholipase and protease enzymes (Lyon & Resende, 2006; Pinto et al., 2008; Zago et al., 2015).

The combined effect of *C. albicans* with other microorganisms may result in synergism and increase the pathogenicity of both microorganisms (Zago et al., 2015; Morales & Hogan, 2010; Peters et al., 2012). It has been estimated that 27% of nosocomial *C. albicans* bloodstream infections are polymicrobial, with *S. aureus* as the third most common isolated organism (Harriott & Noverr, 2009). *S. aureus* is a Gram-positive bacterium and can be found on the skin and mucosa surfaces of human beings (VandenBergh et al., 1999). Studies have described the high prevalence of *S. aureus* on the oral mucosa in denture prosthesis wearers, suggesting that *S. aureus* is a normal colonizer of the oral cavity (Baena-Monroy et al., 2005; Cuesta et al., 2011). In addition, the association between *S. aureus* and *C. albicans* in the colonization of oral mucosa and dental prosthesis wearers with denture stomatitis has been reported (Ribeiro et al., 2012; Baena-Monroy et al., 2005). Not only the microorganisms themselves, but the secreted factors from their metabolisms can promote cell death and inflammatory response in monolayer cell culture (de Carvalho Dias et al., 2017). The secreted factors from the biofilm of mixed-species *C. albicans* and *S. aureus* cultures were more damaging to the monolayer epithelial cells than the secreted factors from the biofilms of single *C. albicans* and *S. aureus* cultures (de Carvalho Dias et al., 2017).

The objectives of this study were to develop and validate a practical and physiologically relevant reconstituted oral mucosa model using immortalized cell lines and to evaluate the developed ROMT as a tool for host-pathogen interaction, both in infected and non-woven tissue exposed to only the secreted factors of single and mixed *C. albicans* and *S. aureus* pathogens.

2. Materials and methods

2.1. ROMT construction

Fibroblasts were obtained from Rio de Janeiro Cell Bank (FGH, cod. 0089), which were derived from human primary cell line established from biopsies of healthy patients' gingiva. Fibroblasts were cultivated in Dulbecco's modified Eagle's medium (DMEM, Gibco, Life

Technologies, USA) supplemented with 10% fetal bovine serum (FBS, Gibco, Life Technologies, USA), antibiotic, antimycotic solution (Sigma, St. Louis, MO, USA). Collagen gel was produced by mixing rat tail collagen type I (First Link (UK) Ltd.) with DMEM, and FBS at 4°C. The solution was neutralized with 1 M NaOH, and a fibroblasts suspension (3.0 x 10 (Dongari-Bagtzoglou & Kashleva, 2006) cells/ml) was added to the mixture. The dermal layer of fibroblast-containing collagen solution was placed in 24 well plates. After 24 h of contraction, the dermal layer was gently removed with the aid of a small spoon immersed in culture medium and washed twice with Hank's Balanced Salt Solution containg calcium and magnesium without phenol red (Gibco, Grand Island, NY). NOK-si keratinocytes were seeded upon the dermal layer (2.0 x 10^6 cells/ml). NOK-si (Castilho et al., 2010) were previously cultivated in DMEM supplemented with 10% FBS and antibiotic antimycotic solution. After NOK-si seeding, tissues were grown until the epithelial cells reached confluence. Then, the neotissues were raised to an air-liquid interface for 14 days in KGM-Gold medium (Lonza, Walkersville, MD USA) supplemented with 0.5 ml hydrocortisone, 0.5 ml transferrin, 0.25 ml epinephrine, 0.5 ml gentamicin sulfate amphotericin-B, 2.0 ml bovine pituitary extract, 0.5 ml epidermal growth factor human and 0.5 ml insulin. The medium was changed every other day. The tissues were prepared in duplicate for each experimental condition and three independent experiments were performed.

2.2. Histological evaluation

The tissues were fixed in 4% formaldehyde buffered at pH 7.2 with 0.1 M sodium phosphate for 24 h at 4°C. Subsequently, the tissues were dehydrated and embedded in paraffin. Four-micron sections were stained with hematoxylin and eosin (HE) and submitted to the periodic acid-Schiff (P.A.S.) histochemical method. Some sections were also stained with Picrosirius-red method and analyzed under light microscope BX-51 (Olympus, Japan) equipped with filters to provide polarized illumination. As control, normal human gingiva was used. Slices of human oral tissue samples were kindly provided by Prof. Dr. Éricka Silveira (Department of Dentistry, Federal University of Rio Grande do Norte-UFRN, Brazil) from the histopathological collection of the institution.

2.3. Immunohistochemical reactions

In the present study, we used the following primary antibodies: rabbit anti-Ki-67 polyclonal antibody (Abcam; ab833, 1/200), rabbit anti-collagen IV polyclonal antibody (Abcam; ab6586, 1/500), rabbit anti-cytokeratin 13 polyclonal antibody (Abcam; ab154346, 1/1000) and mouse anti-cytokeratin 14 monoclonal antibody (Abcam; ab7800, 1/400) (mouse monoclonal). Immunohistochemical reactions were performed using rabbit specific HRP/DAB detection IHC kit (Abcam, ab64261) for Ki-67, collagen IV and cytokeratin 13. The sections were incubated with biotinylated secondary antibody (Dako-K0690; Dako Universal LSAB Kit) for cytokeratin 14.

Tissue sections (4 μm) were deparaffinized, rehydrated and submitted to heat-induced epitope retrieval by microwave treatment for 2 x 5 min in 0.001 M sodium citrate buffer (pH 6.0) (Ki-67, collagen IV and cytokeratin 14), or trypsin/0.1% calcium chloride (cytokeratin 13). After washing with Phosphate-buffered saline - PBS (pH 7.3), sections were treated with 5% hydrogen peroxide (H_2O_2) to block endogenous peroxidase for 10 min at room temperature. After washing, the sections were incubated for 20 min with 2% bovine serum albumin (BSA) and sodium azide/triton at room temperature. Then sections were incubated with primary antibody overnight in the humidified chamber at 4° C. Subsequently, the sections were incubated in biotinylated secondary antibody (Abcam) for 20 min at room temperature and streptavidin for 30 min. The reaction was revealed by using 3,3'-diaminobenzidine (DAB) (Dako, Carpinteria, CA, USA) for 3 min and the sections were counterstained with hematoxylin and mounted. For each
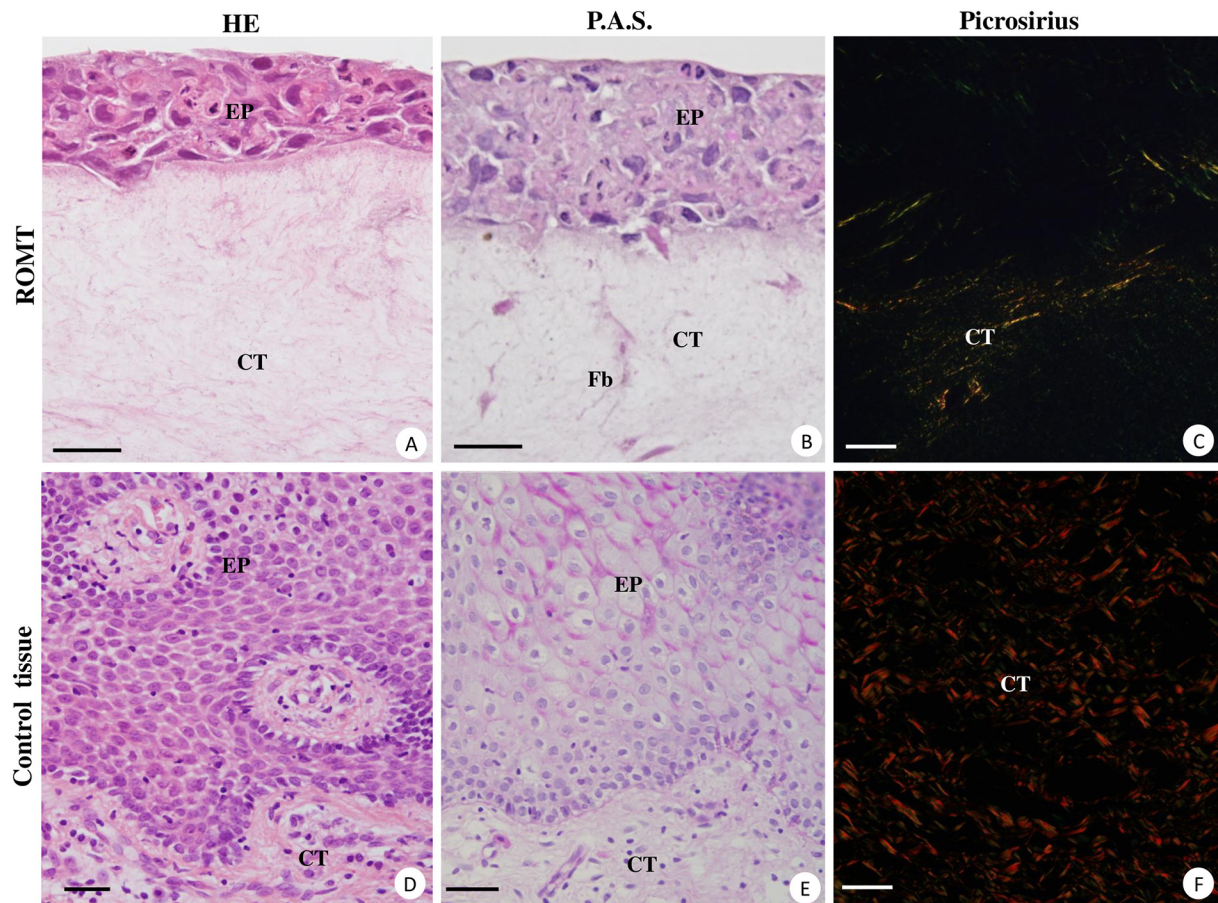
Fig. 1. Light micrographs showing portions of the sections of ROMT (A-C) and human gingival mucosa (D-F). In A and B, the epithelium (EP) exhibits 6–8 layers of cells in close juxtaposition. Note the thick stratified epithelial tissue of human gingiva (D and E). Subepithelial connective tissue (CT) of the ROMT shows few fibroblasts (Fb) and thin collagen fibers whereas several cells are observed in the subepithelial connective tissue (CT) from gingiva (D and E). C and F – sections were stained with Picrosirius-red and analyzed under polarized light. C - Birefringent collagen is present in the subepithelial connective tissue (CT) in the ROMT. F - in the human gingiva several bundles of birefringent collagen fibers are observed distributed throughout the subepithelial connective tissue (CT). Scale Bar: 30 μm. (For interpretation of the references to colour in this figure legend, the reader is referred to the web version of this article.)

sample, a negative control section was performed. In the negative controls, the primary antibody incubation step was replaced by incubation in non-immune serum.

2.4. Ultrastructural characterization

The specimens were examined in a transmission electron microscope (TEM, JEOL JEM-1400) as described previously (Cerri et al., 2009).

2.5. Microbial strains, growth conditions, and tissue infection

C. albicans SC5314 and *S. aureus* ATCC25923 microorganisms were used to produce single and dual species cultures, in accordance with the methodology described by Peters et al. (Peters et al., 2012) and Zago et al. (Zago et al., 2015).

Prior to use, *C. albicans* was maintained in Yeast Peptone Glucose medium (YEPD: 1% yeast extract, 2% Bacto peptone and 2% D-glucose, 2% agar) at -80°C. To prepare stock culture, *C. albicans* was subcultured onto Sabouraud Dextrose Agar plates (SDA-Acumedia Manufactures Inc., Baltimore, MD, USA) supplemented with chloramphenicol (0.05 g/L) and incubated at 37°C for 48 h. A loop full of the agar stock culture was transferred to Yeast Nitrogen Base broth (YNB—Difco, Becton Dickinson Sparks, MD, USA) supplemented with 100 mM glucose and incubated at 37°C overnight (16 h). A 1:10 dilution of the overnight culture was made into fresh YNB supplemented with 100 mM glucose

and allowed to propagate at 37°C until mid-log phase was reached (approximately 8 h).

S. aureus was maintained in Tryptic Soy Broth medium (TSB-Acumedia Manufactures Inc., Baltimore,MD, USA) and frozen at -80°C until use. To prepare stock culture, *S. aureus* was subcultured onto Tryptic Soy Broth medium, and approximately 10 colonies were inoculated into TSB liquid medium overnight (18 h) at 37°C. A 1:20 dilution of the overnight culture was made into fresh TSB and allowed to propagate at 37°C until mid-log phase was reached (approximately 4 h).

Following growth, both microorganisms were washed twice in phosphate-buffered saline (PBS) by centrifugation at 5,000x g for 5 min (rotor model A462), and re-suspended in RPMI 1640 (Sigma-Aldrich, St. Louis, MO, USA) (Dias et al., 2016). *C. albicans* and *S. aureus* suspensions were spectrophotometrically standardized at an OD540 nm of 1.0 and OD600 nm of 0.1, respectively, which corresponds to a final concentration of 1×10^7 cells/mL.

Microorganisms suspensions were placed on top of the reconstituted *in vitro* oral mucosa tissue in antibiotic-free KGM-Gold medium containing growth factors and were incubated in a CO_2 chamber at 37°C. KGM-Gold medium is suitable for microorganism grows (Mohiti-Asli et al., 2014; Mailänder-Sánchez et al., 2017). After 8 and 16 h of incubation, biopsy specimens were collected from infected and uninfected tissues, and stained with hematoxylin and eosin (HE). This infection protocol was compared with the microbe secreted factors protocol (de Carvalho Dias et al., 2017), which after 8 and 16 h of microorganisms cultures in RPMI 1640 (Sigma-Aldrich, St. Louis, MO, USA) (Dias et al.,

2016), the medium was filtered in low protein binding filter (0.2 μm) (SFCA, Corning, Germany) and placed in contact with the tissue for 24 h, under the same conditions.

2.6. Lactate dehydrogenase assay

The release of lactate dehydrogenase (LDH) from tissues into the surrounding medium was monitored as a measure of epithelial cell damage. LDH release into the maintenance media of the cultures containing uninfected and infected epithelial cells (infection and secreted factors protocols) was measured after 8 and 16 h of incubation. LDH activity was analyzed by measuring by fluorescence rate of NADH disappearance at 540 nm excitation and 590 nm emission wavelengths, during the LDH-catalyzed conversion of pyruvate to lactate by using the CytoTox-ONE kit (Promega, G7890) according to the manufacturer's instructions, and FluoroskanAscent FL (Thermo labsystems).

2.7. Statistical analyses

The results of each analysis were tabulated and submitted to normality tests (Shapiro-Wilk) and homogeneity of variance (Levene) to check the distribution of data. Based on the results observed through these tests, we used ANOVA with a significance level of 5%. The values were expressed as the mean and standard deviation of three independent replications, in triplicate for each experimental condition (n = 9).

3. Result

3.1. ROMT construction and characterization

ROMT models using NOK-si cell line and FGH associated with collagen matrix allowed the establishment of a stratified epithelium tissue composed by 6-8 layers of juxtaposed cells (Figs. 1A and B). Although the thickness of the epithelium of ROMT has not reached that observed in the gingival mucosa, the NOK-si cells formed stratified epithelium with similar characteristics to the human gingiva (Figs. 1D and E). Fibroblasts and birefringent collagen fibres showed a structural arrangement forming an intricate network supporting the epithelium (Figs. 1A-F).

Sections of ROMT and gingival mucosa subjected to immunohistochemistry for cytokeratin-13 and -14 detection (epithelial cells markers) exhibited positive immunolabelling in the cytoplasm of epithelial cells (Figs. 2A-D). An enhanced cytokeratin 14 immunolabelling observed in the epithelial cells of different layers in the ROMT (Fig. 2C). In the gingival mucosa, the positive immunoreaction for cytokeratin 14 was particularly observed in the basal and supra basal layers of epithelium (Fig. 2D). In order to investigate the epithelial proliferation, we analyzed Ki-67 immunoexpression in the ROMT and gingival mucosa. Ki-67-positive cells were often found in the stratum basale of the epithelium of ROMT and gingival mucosa (Figs. 2E and F), confirming the occurrence of epithelial cell proliferation in the ROMT.

Based on these findings, the presence of type IV collagen commonly found in the basal lamina was investigated. In ROMT sections, a granular immunopositive material was observed in this region (Fig. 2G). In the gingival mucosa, an evident immunolabelling was detected in the basal lamina (Fig. 2H).

The ultrastructural analysis revealed epithelium composed of several layers of cells in close juxtaposition; numerous desmosomes were observed by attaching a cell to another. These cells exhibited thick tonofilament bundles distributed throughout the cytoplasm (Figs. 3A and B). In the subepithelial connective tissue, some collagen fibrils were also observed (Fig. 3C).

3.2. Tissue damage by C. albicans and S. aureus pathogens and its secreted factors

The ROMT were used to evaluate the potential of single and dual pathogens species to infect and damage the epithelial tissue surface after 8 and 16 h of incubation (Figs. 4 and 5). The results showed that *C. albicans* was able to infect and destroy the ROMT, but *S. aureus* was not. By the methods we performed, single species pathogens of *S. aureus* did not exhibit levels of infection, unlike single species pathogens of *C. albicans*. Invasion of hyphae into epithelium was characterized by tissue destruction. *C albicans* promoted damage in the epithelium surface while the dual species invaded deeply the ROMT cultures reaching the subepithelial collagen matrix. The extent and depth of infection were greater for dual species pathogens (*C. albicans* associated with *S. aureus*) (Fig. 4). After the contact with the pathogens secreted factors, the superficial layer of the ROMT was irregular and altered under all experimental conditions (Fig. 5).

To quantify cell injury, we compared the levels of LDH released after *C. albicans*, *S. aureus* and dual species pathogens (infection and secreted factors protocols) when co-cultured with ROMT. We observed that the amount of LDH released differ greatly between 8 and 16 h of infection. After 8 h of infection, LDH release was low, and single species pathogens of *S. aureus* exhibited the lowest damage. However, after 16 h of infection, a significant increase in the LDH release was found, mainly by dual species pathogens (Fig. 6A). Conversely, after the contact with 8 h pathogens secreted factors caused a significant change in LDH level, without statistical difference between 8 h and 16 h, with the exception of dual pathogens secreted factors that were able to cause more LDH released on 16 h samples (Fig. 6B).

4. Discussion

Our ROMT developed with NOK-si demonstrated to be a practical and stable model during histological examination and provided satisfactory results in ultrastructural analysis. Fibroblasts of lamina propria (connective tissue underlying the epithelium) and epithelial cells (NOK-si) interact to each other and reproduce an oral mucosa with a thick epithelium, which favour the epithelium differentiation. However, the ROMT models did not present flattened keratinized cells in the upper layers, as occurs *in vivo* in some stratified epithelia. Nevertheless, depending on the anatomical region of the oral mucosa, the epithelium may be no-keratinized as floor of the mouth, jugal and labial mucosa and soft palate (Squier & Kremer, 2001). Thus, the ROMT could be used to mimic these structures. In addition, the ROMT developed in this study permitted the assessment of the potential of single and dual species pathogens to infect and cause pathological change of the oral mucosa tissue. Moreover, it could be used as a tool for studies of metabolites, toxins and other molecules derived from pathogens; this was demonstrated in our results.

Various studies have attempted to develop a reconstituted oral tissue as similar as human oral mucosa (Dongari-Bagtzoglou & Kashleva, 2006; Kinikoglu et al., 2009; Yoshizawa et al., 2004). However, most studies have used primary fibroblasts and epithelial cells isolated from human palatal biopsy specimens. In the present study, the ROMT model was constructed by seeding NOK-si keratinocytes on gingival fibroblasts embedded in a collagen matrix and showed a well-organized and stratified tissue with a structural organization similar to human oral mucosa, which was used as a control. NOK-si cells were used because they maintain epithelial morphology, proliferative capacity, and the expression of typical markers such as cytokeratins and Ecadherin (Castilho et al., 2010).

Our findings showed a similar pattern of immunolabelling in the ROMT with NOK-si cells and gingival mucosa. We observed Ki-67-immunolabeled cells in the ROMT, which indicate maintenance of active cell proliferation in the basal and suprabasal layers, consistent with turnover found in the stratified epithelia Dongari-Bagtzoglou,
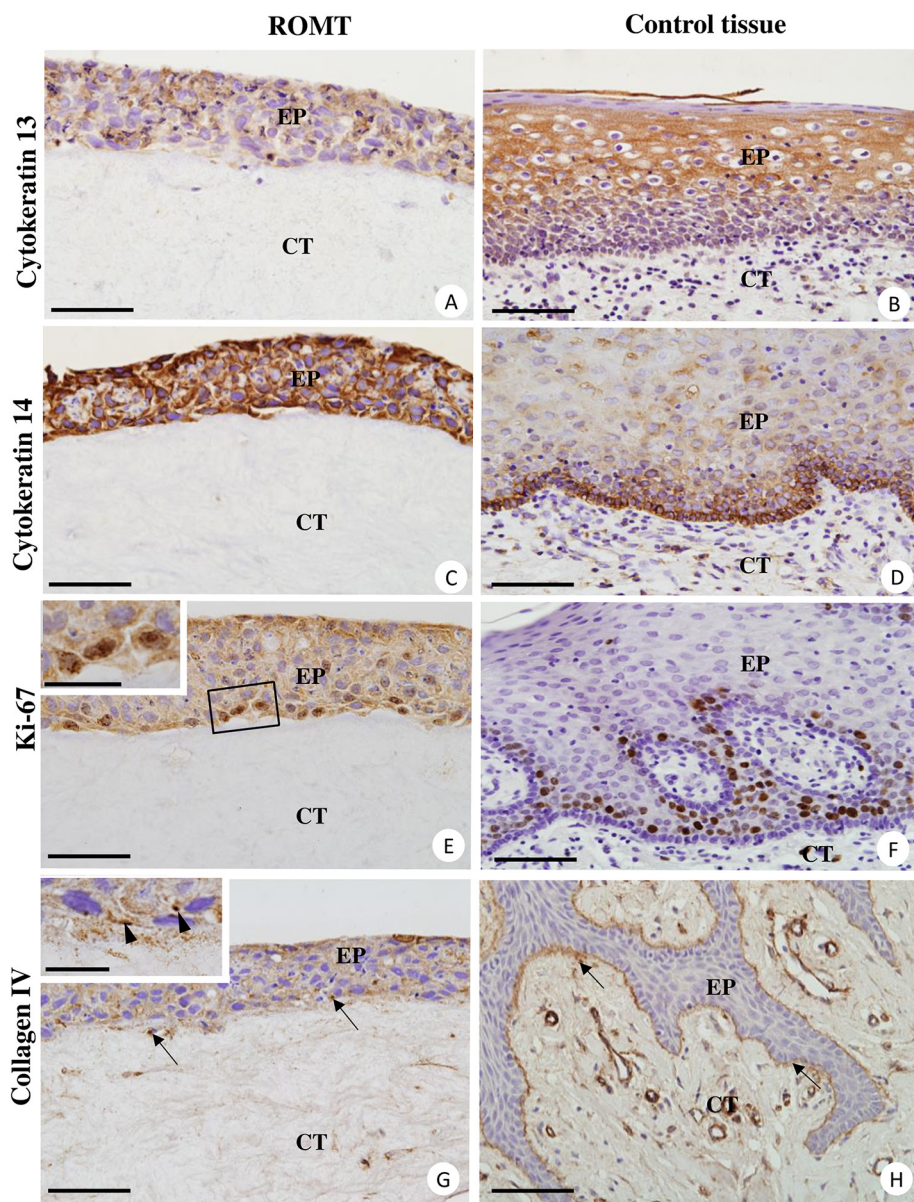
ROMT

Control tissue

Fig. 2. Light micrographs showing portions of sections of ROMT (A, C, E and G) and human gingival mucosa (B, D, F and H). A and B images show the immunoexpression for cytokeratin 13 (brown-yellow colour) in the epithelial tissues (EP). The ROMT exhibits immunolabeled cells in the different layers of the epithelium while in the human gingiva the immunoexpression is present in the middle and in the superficial layers of epithelium (EP). C and D images show strong cytokeratin 14 immunolabeling in epithelial cells is observed in the ROMT. Note that in the human gingiva immunostaining is evident in the basal stratum. E and F – Ki-67-immunopositive nucleus are observed in the basal stratum of the epithelia of ROMT and human gingiva. The inset of the outlined area in E shows strong Ki-67-immunopositive cells in the basal stratum of ROMT. G and H – a delicate collagen IV immunolabeling (arrows – G) is observed between epithelial (EP) and connective tissues (CT) in the ROMT. The inset shows granular immunopositive material in the epithelium-connective interface. Epithelial cells exhibit immunopositive cytoplasm (arrowheads). H - A conspicuous immunostaining (arrows) is observed in the basal lamina of the human gingiva. Scale Bar: 45 μm; inset (E and G): 20 μm. (For interpretation of the references to colour in this figure legend, the reader is referred to the web version of this article.)
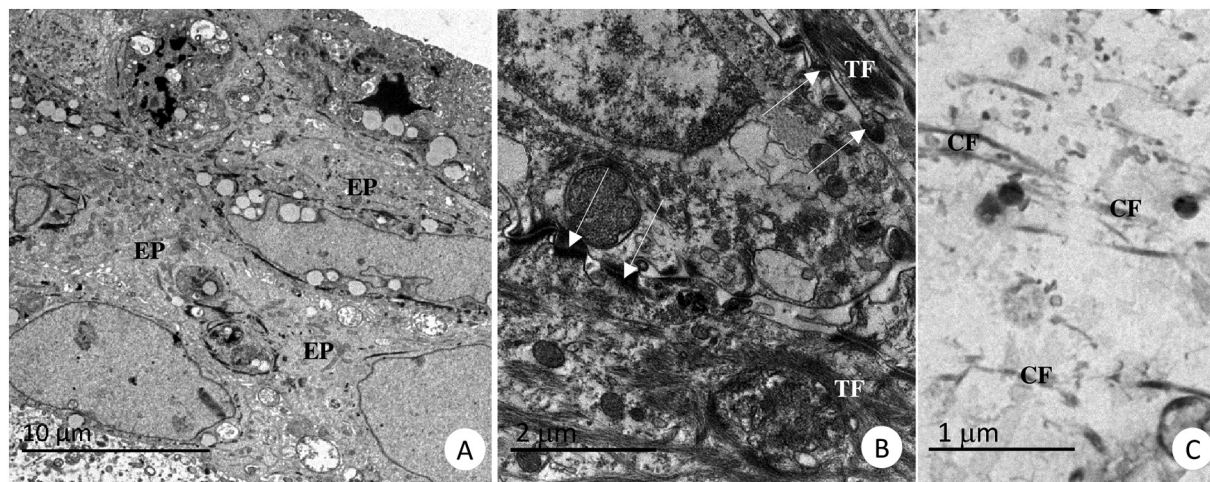

Fig. 3. Electron micrographs of ROMT. A) Epithelium tissue shows several layers of cells (EP) in close juxtaposition. B) desmosomes junctions (arrows) are observed between adjacent epithelial cells. Bundles of tonofilaments (TF) are distributed throughout the cytoplasm of epithelial cells. C) a portion of the connective tissue showing some collagen fibrils (*CF*) surrounded by amorphous material.
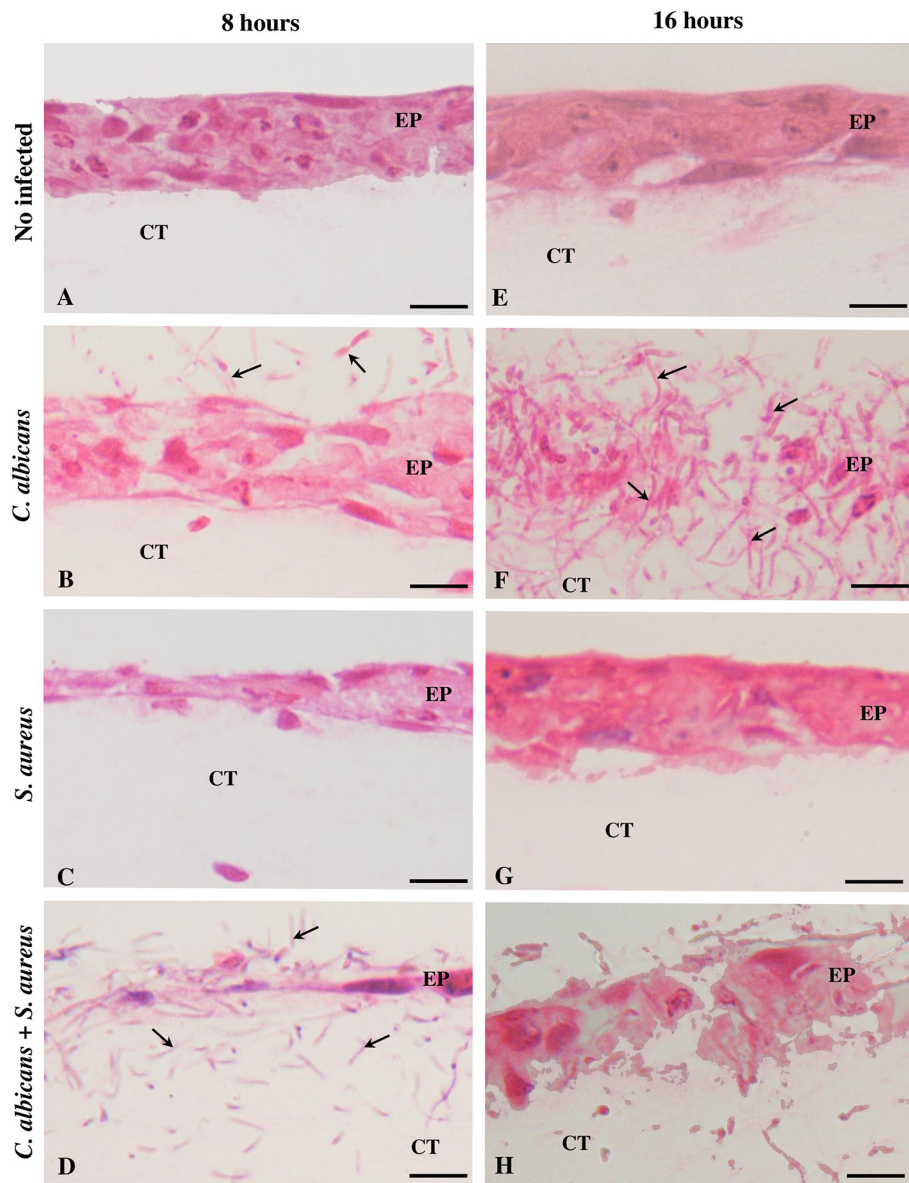
Fig. 4. Light micrographs showing sections of ROMT infected with single-species pathogens (*C. albicans* alone or *S. aureus* alone) and dual-species pathogens (*C. albicans* associated with *S. aureus*) after 8 (Fig. 4A-D) and 16 h (Fig. 4E-H). EP: epithelium; CT: subepithelial connective tissue; arrows: hyphae. HE. Bars: 20 μm.

A.[5],Kinikoglu, B., 2009, Yoshizawa, M., 2004[30,31]. However, while in these studies human fibroblasts and primary oral keratinocytes were used to create a culture system to produce oral mucosa equivalents, immortalized cell lines were used in the experiments in the present investigation.

Cytokeratin 13 showed strong suprabasal immunoexpression in the control oral mucosa, with basal layers of the epithelium being negative. Similarly, the ROMT also showed expression of cytokeratin 13. These results are in agreement with those previously shown by other authors (Garzón et al., 2009; de Carvalho Dias et al., 2017).

Cytokeratin 14 immunoexpression is usually present in the basal and supra-basal strata of stratified epithelia (Dabija-Wolter et al., 2013; Rao et al., 2014). The strong immunolabeling for cytokeratin 14 was observed in all the layers of the stratified epithelium from ROMT may be due to an activated state of migrating epithelial cells. On the other hand, cytokeratin 14 was mainly expressed in basal epithelial cells of the control tissue, which may represent cells in a low proliferative state. These findings are in accordance with others studies that also reported the immunolabeling for cytokeratin 14 throughout the stratified

epithelium in human oral mucosa models (Oksanen & Hormia, 2002; Rouabhia & Allaire, 2010).

The type IV collagen is a typical protein present of the basal lamina synthetized by epithelial cells (Becker et al., 1986). In the ROMT, the immunolabeling for collagen IV was observed between epithelium and collagen matrix, i.e., in the region correspondent to basal lamina. Although the immunolabeled material was sparsely distributed in this region, epithelial cells exhibiting immunolabeled cytoplasm were also observed reinforced the idea that the epithelial cells of ROMT can produce the collagen IV. A weak immunoexpression for collagen IV was also found in multilayered three-dimensional organotypic culture models (Dabija-Wolter et al., 2013).

Ultrastructural analysis revealed the presence of bundles of tonofilaments in the cytoplasm of cells of the reconstituted epithelium, as described in the epithelial cells (Cerri et al., 2009). Moreover, numerous desmosomes promoting intercellular connections, similar to the observed in oral epithelium was found in the epithelium of ROMT. Subjacent to the stratified epithelium, few fibroblasts and some collagen fibrils intermingle to amorphous material formed the scaffold
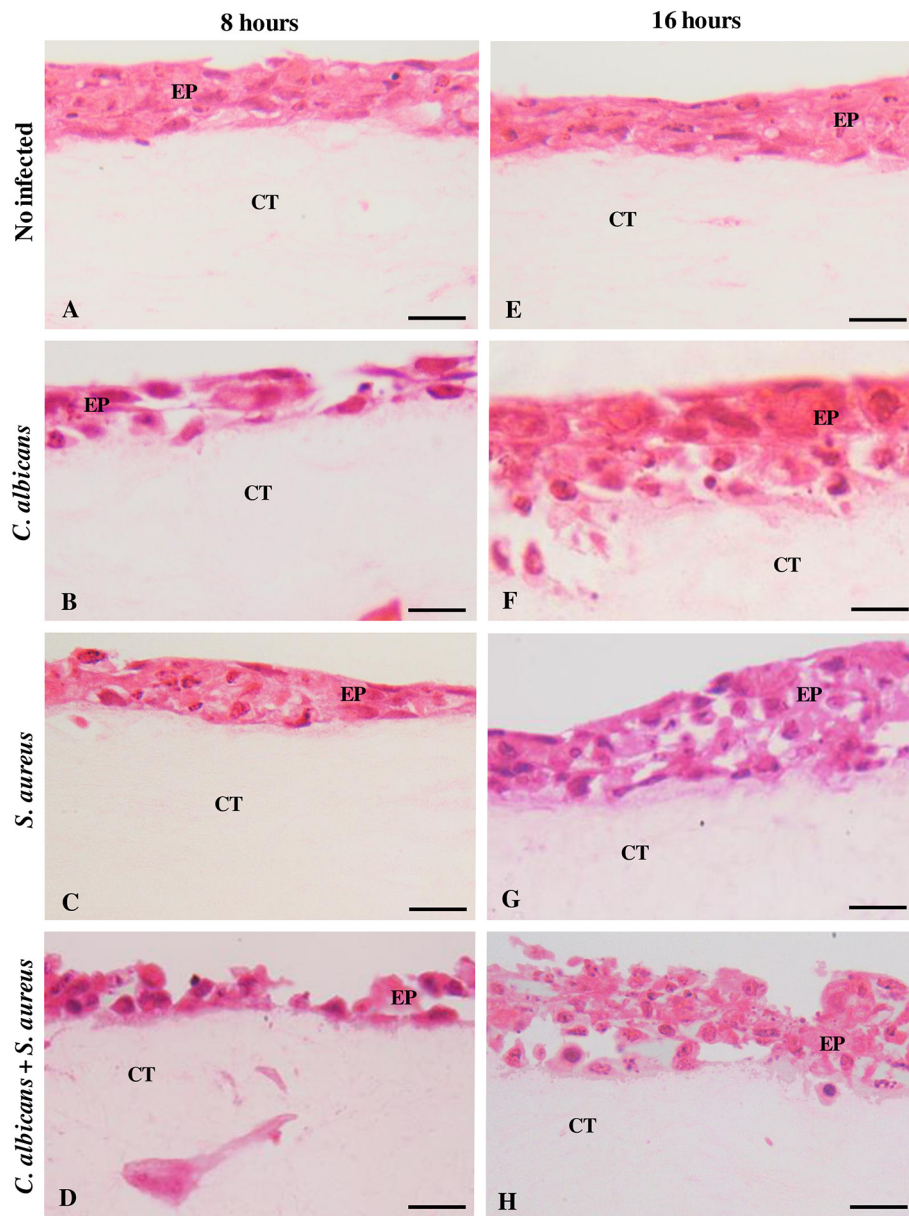
Fig. 5. Light micrographs showing portions of sections of ROMT exposed to single-species pathogens secreted factors (*C. albicans* alone or *S. aureus* alone) and dual-species pathogens secreted factors (*C. albicans* associated with *S. aureus*) after 8 (Figs. 5A-D) and 16 h (Fig. 5E-H) exposure. EP: epithelium; CT: subepithelial connective tissue. HE. Bars: 20 μm.

which allowed the epithelial cell proliferation and well-organized re-constituted epithelium tissue.

Single species and dual species pathogens were able to induce structural modifications on ROMT developed, with greater alterations caused by *C. albicans*. However, the extent and depth of infection were greater for dual species pathogens (*C. albicans* associated with *S. aureus*). Our results are consistent with literature (Zago et al., 2015; Peters et al., 2012; Schlecht et al., 2015). Peters et al. (Zago et al., 2015) assessed the potential implications of interaction between either species alone (*C. albicans* and *S. aureus*) or co-infected with host and a lack of inflammatory infiltrates was confirmed with a non-invasive presence of *S. aureus* on the tissue; the association of staphylococcal cells with *C. albicans* hyphae, as they penetrate host tissue, may allow *S. aureus* to gain entry into deeper tissues and initiate infection, with dire consequences for the host, particularly in critically ill patients. Evidence indicates that *S. aureus* and *C. albicans* are able to form a dense poly-microbial biofilm on the epithelial surface with or without the

expression of protein agglutinin-like sequence 3 (Als3p). However, *S. aureus* is unable to enter the bloodstream and disseminate in the absence of Als3p, ostensibly due to the lack of binding to penetrating hyphae (Schlecht et al., 2015).

The morphological analysis revealed that *S. aureus* caused the least damage and had the lowest LDH levels, although significantly greater than the uninfected control. On the other hand, the dual species pathogens had the highest level of the LDH and tissue damage. These findings suggest that *C. albicans* can facilitate the damaging of *S. aureus* (Schlecht et al., 2015), since *S. aureus* typically requires a breach in host surface barriers to invade (Acton et al., 2009), which may be caused by *C. albicans*. Zago et al. (Zago et al., 2015) found high production of proteinase in single *S. aureus* biofilm, while single *C. albicans* biofilm presented high phospholipase levels. However, when both microorganisms were co-cultured, both enzymes were produced. Furthermore, proteomic analysis showed that a total of 27 proteins were significantly differentially produced by *S. aureus* and *C. albicans* during co-
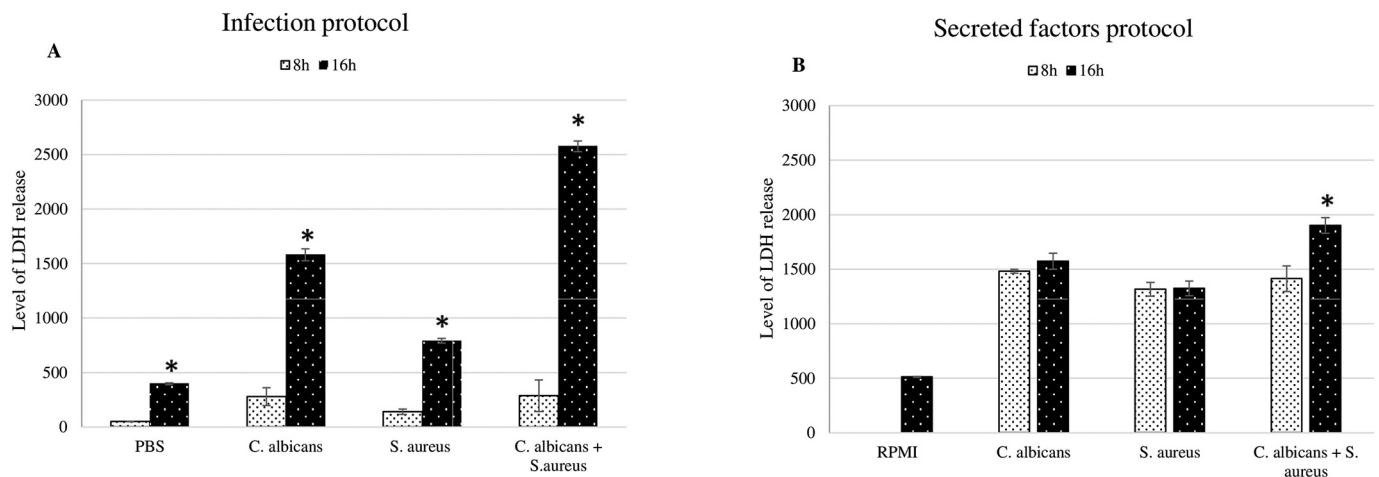
Fig. 6. LDH released from ROMT infected with single- (*C. albicans* alone and *S. aureus* alone) and dual-species pathogens (*C. albicans* associated with *S. aureus*) (A) or exposed to single- and dual-species pathogens secreted factors (B) after 8 and 16 h. Results are the mean ± SD of three experiments, each condition set up in triplicate. Error bars represent SD ($n = 9$ replicates).*$p \leq .05$. All experimental groups (*C. albicans* alone, *S. aureus* alone or *C. albicans* associated with *S. aureus*) were statistically different from the control group (PBS or RPMI).

culture biofilm growth (Peters et al., 2010). Both single and dual 8h and 16h pathogens secreted factors resulted in LDH released and changes in the morphology of ROMT. However, the 16h dual pathogens secreted factors resulted in more tissue damage. The results show that the response in the developed ROMT, as well as occurs *in vivo*, may differ according to the experimental/clinical conditions. The findings of this, indicate a level of differentiation within the optimized ROMT and show that it is possible to use this tissue as a tool for host-pathogen interactions.

5. Conclusion

The results provide clear indications towards a reproducible and relevant *in vitro* model for investigations of oral mucosa infections and may be a useful adjunct to pre-clinical studies of oral disease progression and for studying virulence factors.

Acknowledgement

References

Acton, D.S., Plat-Sinnige, M.J., van Wamel, W., de Groot, N., van Belkum, A., 2009. Intestinal carriage of *Staphylococcus aureus*: how does its frequency compare with that of nasal carriage and what is its clinical impact? Eur J Clin Microbiol Infect Dis. 28 (2), 115–127.

Baena-Monroy, T., Moreno-Maldonado, V., Franco-Martínez, F., Aldape-Barrios, B., Quindós, G., Sánchez-Vargas, L.O., 2005. Candida albicans, *Staphylococcus aureus* and *Streptococcus mutans* colonization in patients wearing dental prosthesis. Med Oral Patol Oral Cir Bucal. 10 (Suppl 1), E27–E39.

Becker, J., Schuppan, D., Hahn, E.G., Albert, G., Reichart, P., 1986. The immunohistochemical distribution of collagens type IV, V, VI of and laminin in the human oral mucosa. Arch Oral Biol. 31 (3), 179–186.

Boelsma, E., Verhoeven, M.C., Ponec, M., 1999. Reconstruction of a human skin equivalent using a spontaneously transformed keratinocyte cell line (HaCaT). J Invest Dermatol. 112 (4), 489–498.

Brohem, C.A., Cardeal, L.B., Tiago, M., Soengas, M.S., Barros, S.B., Maria-Engler, S.S., 2011. Artificial skin in perspective: concepts and applications. Pigment Cell Melanoma Res. 24 (1), 35–50.

Castilho, R., Squarize, C.H., Leelahavanichkul, K., Zheng, Y., Bugge, T., Gutkind, J.S., 2010. Rac1 is required for epithelial stem cell function during dermal and oral mucosa wound healing but not for tissue homeostasis in mice. PLos One. 6;5(5):e10503.

Cerri, P.S., Gonçalves, J. de S., Sasso-Cerri, E., 2009. Area of rests of Malassez in young and adult rat molars: evidences in the formation of large rests. Anat Rec (Hoboken). 292 (2), 285–291.

Coronado-Castellote, L., Jiménez-Soriano, Y., 2013. Clinical and microbiological diagnosis of oral candidiasis. Journal of Clinical and Experimental Dentistry. 5 (5), e279–e286.

Cuesta, A.I., Jewtuchowicz, V.M., Brusca, M.I., Mujica, M.T., Rosa, A.C., 2011. Antibiotic susceptibility of *Staphylococcus aureus* isolates in oral mucosa and pockets of patients with gingivitis-periodontitis. Acta Odontol Latinoam. 24 (1), 35–40.

Dabija-Wolter, G., Bakken, V., Cimpan, M.R., Johannessen, A.C., Costea, D.E., 2013. In vitro reconstruction of human junctional and sulcular epithelium. J Oral Pathol Med. 42 (5), 396–404.

de Carvalho Dias, K., Barbugli, P.A., de Patto, F., Lordello, V.B., de Aquino Penteado, L., Medeiros, A.I., Vergani, C.E., 2017. Soluble factors from biofilm of *Candida albicans* and *Staphylococcus aureus* promote cell death and inflammatory response. BMC Microbiol. 17 (1), 146.

Dias, K.C., Barbugli, P.A., Vergani, C.E., 2016. Influence of different buffers (HEPES/MOPS) on keratinocyte cell viability and microbial growth. J Microbiol Methods. 25, 40–42.

Dongari-Bagtzoglou, A., Kashleva, H., 2006. Development of a highly reproducible three-dimensional organotypic model of the oral mucosa. Nature protocols. 1 (4), 2012–2018.

Edmondson, R., Broglie, J.J., Adcock, A.F., Yang, L., 2014. Three-dimensional cell culture systems and their applications in drug discovery and cell-based biosensors. Assay Drug Dev Technol. 12 (4), 207–218.

Finkel, J.S., Mitchell, A.P., 2011. Genetic control of *Candida albicans* biofilm development. Nat Rev Microbiol. 9, 109–118.

Garcia, M.C., Lee, J.T., Ramsook, C.B., Alsteens, D., Dufrêne, Y.F., Lipke, P.N., 2011. A role for amyloid in cell aggregation and biofilm formation. PLoS One. 6 (3), e17632.

Garzón, I., Sánchez-Quevedo, M.C., Moreu, G., González-Jaranay, M., González-Andrades, M., Montalvo, A., Campos, A., Alaminos, M., 2009. In vitro and in vivo cytokeratin patterns of expression in bioengineered human periodontal mucosa. J Periodontal Res. 44 (5), 588–597.

Harriott, M.M., Noverr, M.C., 2009. *Candida albicans* and *Staphylococcus aureus* form polymicrobial biofilms: effects on antimicrobial resistance. Antimicrob Agents Chemother. 53 (9), 3914–3922.

Jacobsen, I.D., Wilson, D., Wächtler, B., Brunke, S., Naglik, J.R., Hube, B., 2012. *Candida albicans* dimorphism as a therapeutic target. Expert Rev Anti Infect Ther. 10 (1), 85–93.

Kehe, K., Abend, M., Kehe, K., Ridi, R., Peter, R.U., van Beuningen, D., 1999. Tissue engineering with HaCaT cells and a fibroblast cell line. Arch Dermatol Res. 291 (11), 600–605.

Kinikoglu, B., Auxenfans, C., Pierrillas, P., Justin, V., Breton, P., Burillon, C., Hasirci, V., Damour, O., 2009. Reconstruction of a full-thickness collagen-based human oral mucosa equivalent. Biomaterials. 30 (32), 6418–6425.

Lyon, J.P., Resende, M.A., 2006. Correlation between adhesion, enzyme production, and susceptibility to fluconazole in *Candida albicans* obtained from denture wearers. Oral Med Oral Pathol Oral Radiol Endod. 102, 632–638.

Mailänder-Sánchez, D., Braunsdorf, C., Grumaz, C., Müller, C., Lorenz, S., Stevens, P., Wagener, J., Hebecker, B., Hube, B., Bracher, F., Sohn, K., Schaller, M., 2017. Antifungal defense of probiotic Lactobacillus rhamnosus GG is mediated by blocking adhesion and nutrient depletion. PLoS One. 12 (10), e0184438.

Mayer, F.L., Wilson, D., Hube, B., 2013. *Candida albicans* pathogenicity mechanisms. Virulence. 4 (2), 119–128.

Mohiti-Asli, M., Pourdeyhimi, B., Loboa, E.G., 2014. Skin tissue engineering for the infected wound site: biodegradable PLA nanofibers and a novel approach for silver ion release evaluated in a 3D coculture system of keratinocytes and *Staphylococcus aureus*. Tissue Eng Part C Methods. 20 (10), 790–797.

Morales, D.K., Hogan, D.A., 2010. *Candida albicans* interactions with bacteria in the context of human health and disease. PLoS Pathog. 29; 6(4):e1000886.

Oksanen, J., Hormia, M., 2002. An organotypic in vitro model that mimics the dento-epithelial junction. J Periodontol. 73 (1), 86–93.

Peters, B.M., Jabra-Rizk, M.A., Scheper, M.A., Leid, J.G., Costerton, J.W., Shirtliff, M.E., 2010. Microbial interactions and differential protein expression in *Staphylococcus aureus -Candida albicans* dual-species biofilms. FEMS Immunol Med Microbiol. 59 (3), 493–503.

Peters, B.M., Jabra-Rizk, M.A., O'May, G.A., Costerton, J.W., Shirtliff, M.E., 2012. Polymicrobial interactions: impact on pathogenesis and human disease. Clinical Microbiology Reviews. 25 (1), 193–213.

Pinto, E., Ribeiro, I.C., Ferreira, N.J., Fortes, C.E., Fonseca, P.A., Figueiral, M.H., 2008. Correlation between enzyme production, germ tube formation and susceptibility to fluconazole in *Candida* species isolated from patients with denture-related stomatitis and control individuals. J Oral Pathol Med. 37, 587–592.

Rao, R.S., Patil, S., Ganavi, B.S., 2014. Oral cytokeratins in health and disease. J Contemp Dent Pract. 15 (1), 127–136.

Ribeiro, D.G., Pavarina, A.C., Dovigo, L.N., Machado, A.L., Giampaolo, E.T., Vergani, C.E., 2012. Prevalence of *Candida* spp. associated with bacteria species on complete dentures. Gerodontology. 29 (3), 203–208.

Rouabhia, M., Allaire, P., 2010. Gingival mucosa regeneration in athymic mice using in vitro engineered human oral mucosa. Biomaterials 31 (22), 5798–5804.

Scheller, E.L., Krebsbach, P.H., Kohn, D.H., 2009. Tissue engineering: state of the art in oral rehabilitation. J Oral Rehabil. 36 (5), 368–389.

Schlecht, L.M., Peters, B.M., Krom, B.P., Freiberg, J.A., Hänsch, G.M., Filler, S.G., Jabra-Rizk, M.A., Shirtliff, M.E., 2015. Systemic *Staphylococcus aureus* infection mediated by *Candida albicans* hyphal invasion of mucosal tissue. Microbiology. 161 (Pt 1), 168–181.

Shirtliff, M.E., Peters, B.M., Jabra-Rizk, M.A., 2009. Cross-kingdom interactions: *Candida albicans* and bacteria. FEMS Microbiol Lett. 299 (1), 1–8.

Squier, C.A., Kremer, M.J., 2001. Biology of oral mucosa and esophagus. J Natl Cancer Inst Monogr. (29), 7–15.

VandenBergh, M.F., Yzerman, E.P., vvan Belkum, A., Boelens, H.A., Sijmons, M., Verbrugh, H.A., 1999. Follow-up of *Staphylococcus aureus* nasal carriage after 8 years: redefining the persistent carrier state. J Clin Microbiol. 37 (10), 3133–3140.

Yoshizawa, M., Feinberg, S.E., Marcelo, C.L., Elner, V.M., 2004. Ex vivo produced human conjunctiva and oral mucosa equivalents grown in a serum-free culture system. J Oral Maxillofac Surg. 62 (8), 980–988.

Zago, C.E., Silva, S., Sanitá, P.V., Barbugli, P.A., Dias, C.M., Lordello, V.B., Vergani, C.E., 2015. Dynamics of biofilm formation and the interaction between *Candida albicans* and methicillin-susceptible (MSSA) and -resistant *Staphylococcus aureus* (MRSA). PLoS One. 13, 10(4).